NISS

Permeability of Cracked Concrete

Kejin Wang, Daniel C. Jansen, Surendra P. Shah,
and Alan F. Karr

Technical Report Number 46
August, 1996

National Institute of Statistical Sciences
19 T. W. Alexander Drive
PO Box 14006
Research Triangle Park, NC 27709-4006
www.niss.org

PERMEABILITY STUDY OF CRACKED CONCRETE

Kejin Wang, Daniel C. Jansen, Surendra P. Shah
The NSF Center for Advanced Cement-Based Materials
Northwestern University
2145 Sheridan Rd., Evanston
Illinois 60208-4400, USA

and

Alan F. Karr
National Institute of Statistical Sciences
PO Box 14162, Research Triangle Park
North Carolina 27709-4162, USA

ABSTRACT

Cracks in concrete generally interconnect flow paths and increase concrete permeability. The increase in concrete permeability due to the progression of cracks allows more water or aggressive chemical ions to penetrate into the concrete, facilitating deterioration. The present work studies the relationship between crack characteristics and concrete permeability. In this study, feedback controlled splitting tests are introduced to generate crack width-controlled concrete specimens. Sequential crack patterns with different crack widths are viewed under microscope. The permeability of cracked concrete is evaluated by water permeability tests. The preliminary results indicate that crack openings generally accelerate water flow rate in concrete. When a specimen is loaded to have a crack opening displacement smaller than 50 microns prior to unloading, the crack opening has little effect on concrete permeability. When the crack opening displacement increases from 50 microns to about 200 microns, concrete permeability increases rapidly. After the crack opening displacement up to 200 microns, the rate of water permeability increases steadily. The present research may provide insight in developing design criteria for a durable concrete and in predicting service life of a concrete structure.

Introduction

Concrete deterioration is greatly related to its permeability. Most researchers believe that a well designed and manufactured concrete is originally a water-tight material, containing discontinuous pores and microcracks. When subjected to extreme loading or weathering, concrete deteriorates through a variety of physical and chemical processes, resulting in cracking. Cracks in concrete generally interconnect flow paths and increase concrete permeability. The increase in concrete permeability due to crack progression allows more water or aggressive chemical ions to penetrate into concrete, facilitating further deterioration. Such a chain reaction of "deterioration -- cracking -- more permeable concrete -- further deterioration" may eventually result in destructive deterioration of the concrete structure (1). Therefore, it is significant to understand the mutual interaction and relationship between concrete cracks and its permeability.

Due to difficulties in generating desirable crack patterns in concrete specimens and availability of appropriate methods for concrete permeability measurements, limited study has been done on permeability of cracked concrete. Some related research has been conducted on permeability of the concrete subjected to compressive loading. It was reported that the application of compressive loads had little effect on both chloride and water permeability of concrete although some evidence indicates that significant microcraking occurred in the concrete (2, 3). These results seem to contradict the widely accepted holistic model that shows the chain reaction of concrete deterioration above (1). Since crack characteristics were not studied in the previous research, it is not clear whether the results are related to the loading methods or the permeability measurements. It is possible that crack openings generated under loading may recover significantly after unloading; thus resulting in an insignificant increase in connected flow paths in concrete. For the concrete having excessively wide and connected cracks, it is not clear whether the rapid chloride permeability test is still suitable for permeability measurement because the specimen may heat up quickly and the sodium chloride and sodium hydroxide solutions used in the test may mix through the cracks. It seems desirable to study permeability of cracked concrete by generating cracks in tension and taking water permeability measurements.

Tsukamoto (5) measured the rate of water flows in plain and fiber reinforced concrete specimens under uniaxial tension. In this study, slab-shaped specimens were used for the uniaxial tensile loading, and notches were made on the sides of the specimens for producing cracks in the middle of the specimens. Due to the shape of the specimens, one-directional water flow was not achieved, and calculation of the concrete permeability coefficient became complicated. A more appropriate testing method is needed to study permeability of cracked concrete.

In the present research, feedback controlled splitting tests are introduced to generate width-controlled cracks in concrete specimens. This testing method has several advantages: 1) cracks are produced by tensile stresses, 2) crack opening displacement is recorded during loading and after unloading, and 3) the cylindrical specimens used in the loading tests are preferable for conventional concrete permeability tests. After the splitting tests, sequential crack patterns were viewed under an optical microscope. Water permeability of the cracked concrete specimens was evaluated. Studying the relationship between crack characteristics and concrete permeability, the present research provides insight in developing design criteria for a durable concrete, predicting service life of a concrete structure, and determining repair strategies and methods for deteriorated concrete.

Experimental Program

Concrete specimens were 25 mm (1 in.) thick slices, cut from 100mm x 200mm (4in x 8in) cylinders. By means of the feedback controlled splitting tests, the specimens were loaded to have a crack opening displacement of 25, 50, 80, 110, 140, 180, 350, or 550 microns. After unloading, the crack patterns of some of the specimens were examined under an optical microscope. Then, water permeability of the specimens was tested.

Concrete Mix Proportion and Properties

The concrete mix proportion used in the present study is shown in Table 1. The water/cement ratio of the mix was 0.41 (by weight). The slump of the fresh concrete was 3.2 cm (1.25 in.). The specimens were cured under water, in a room with a temperature of 20 °C, for about 90-100 days before being subjected to splitting tests and permeability tests. The 28-day compressive strength of the concrete was 45 MPa (6500 psi).

Table 1 -- Mix Proportion of Concrete

Materials	Mix Proportion	
	(kg/m^3)	(lb/yd^3)
Cement (Type I)	344	579
Water	195	328
Pea Gravel (oven dry) (MSA=9 mm or 3/8")	1036	1743
River Sand (oven dry) (F.M.=2.6)	858	1444

Feedback Controlled Splitting Tests

The feedback controlled splitting test is a Brazilian splitting test controlled by a closed-loop feedback system. Closed-loop test machines function by adjusting the actuator (loading ram) to get a desired value from a measured parameter or a feedback signal. This measured parameter could be force or stroke, although for these tests it was the average displacement measured by the lateral LVDTs. By continuously increasing the desired value, the value of the feedback measurement is also increased even if the load carrying capacity of the specimen decreases (6). The test setup is shown in Figure 1. A cylindrical specimen (100 mm in diameter and 25 mm in thickness) was loaded diametrically under Brazilian test configuration. A single LVDT was fixed on each side of the specimen, perpendicular to the loading direction, so as to monitor the crack opening displacement (COD). The LVDTs each had a range of ±0.5 mm. Plywood strips, 25 mm wide and 3 mm in thickness, were placed between the loading plates and the specimen to prevent crushing at the loading points. The 4.4 MN test machine (one million pound) was used with a 490 kN strain gage load cell to measure the force (a calibrated range of 49 kN was used for the 25 mm thick specimens). The average displacement of the two LVDTs was digitally calculated and used as the feedback control. The control parameter, the average crack opening displacement, was increased at a constant rate of 0.2 μm/sec. The specimens were loaded to a predetermined crack width under the feedback controlled condition; and then, unloaded under force control. The time, force, stroke, and crack opening displacement from each LVDT as well as their average (used as the feedback signal) were recorded during tests.

The test results were plotted by a curve of the average displacement of the two LVDTs as a function of tensile stress. The stress is defined as $\sigma = 2P/\pi LD$, where σ is the tensile stress perpendicular to the loading direction along the diameter from one load point to the other, P is the force applied to the specimen, L is the specimen length or thickness, and D is the specimen diameter.

Figure 1 Feedback Controlled Splitting Test Setup

Permeability Tests

Water permeability tests were performed on the cracked specimens. The testing procedure includes specimen vacuuming and saturation, test setup, and permeability measurement (3).

Specimen Vacuuming and Saturation

The vacuuming and saturation followed the sample preparation for rapid chloride permeability tests (AASHTO T277). The specimens were first vacuumed in a desiccator for 3 hours. De-aired water was added, and the specimens were vacuumed under water for another hour. The de-aired water was obtained from boiling de-ionized water for 2 hours and cooling to room temperature. After saturated vacuum, the specimens were left in the desiccator and soaked for at least 12 hours.

Test Setup

After removed from the desiccator, the centers of specimen were covered with a piece of rubber disc, 75 mm (3 in.) in diameter and 1.6 mm (1/16 in.) thick, on both top and bottom surfaces. The rest of specimen surface was dried with a paper towel and coated with fast-setting epoxy. The purpose of this procedure was to prevent moisture loss of the specimen during specimen preparation.

Figure 2 Schematic View of Water Permeability Apparatus

The specimen was then mounted and clamped as shown in Figure 2. Two plexiglas rings, with 76 mm (3 in.) inside diameter, 5 mm (3/16 in.) thick, and 25 mm (1 in.) high, were mounted on the top and bottom surface of the specimen with silicon rubber. A 12 mm x 138 mm x138 mm (0.5 in. x 5.5 in. x 5.5 in.) plexiglas plate with a pipet was mounted on the top plexiglas ring immediately after the rubber disc was removed, and another, with a drain tube, was placed on the bottom ring. Four threaded bars were used to clamp the cell together. The specimen circumferencial surface and all connections were re-sealed with silicon rubber to ensure there would be no leaking of water. After the silicon rubber set, the cells were filled with de-ionized water both above and below the specimen.

Permeability Measurement

The water permeability test started with the filling of the pipette with water. The water permeated from top to the bottom due to the pressure head, which was about 300 mm (1 ft.) of water. The water drop was measured at regular time intervals, normally once a day, depending on the water flow rate of the specimen. After each measurement, water was restored to the original level by refilling the pipette with a syringe from top. The test results were plotted with a curve of the cumulative water flow versus time. Previous studies have shown that after about 7 days, the curve becomes linear (3), which indicates that a steady state flow is established and Darcy's law can be applied to the permeability analysis. As a result, in the present study, most specimens were tested for 20 days and a few were tested for 50 days to ensure that steady state flow was achieved.

The coefficient of permeability (k, in cm/sec) based on Darcy's law for a falling water head can be calculated according to the following equations (4):

$$\frac{dQ}{dt} = -\frac{A'\,dh}{dt} = k\frac{h}{L}A$$

$$-\frac{dh}{h} = k\frac{hA}{A'L}dt$$

Integrating from h_o to h_1:

$$k = \frac{A'L}{At}\ln\frac{h_0}{h_1}$$

Here, A' is the cross sectional area of pipette (0.5 cm^2); A, cross sectional area of specimen (cm^2); h_0 and h_1 are initial and final water heads (cm); L is the specimen thickness (cm); Q is the volume of water flow (cm^3); and t is time (sec).

Results and Discussion

Feedback Controlled Splitting Tests

The results from the feedback controlled splitting tests are shown in Figure 3. It was observed that the peak load generally occurred at an average transverse displacement of about 20 microns.

The peak stress, or the tensile strength, was about 6 MPa. After passing the peak stress, the load was reduced due to the initiation of cracks in concrete.

Figure 3 Results from Feedback Controlled Splitting Tests

The data from the two LVDTs showed that the cracks generally opened on one face first and on the other face later. This means that to guarantee a stable feedback control, it is essential to use a combination of the lateral displacements measured on both faces as the feedback signal. When the load dropped down to about 75% of the peak load, it remained constant as the displacement increased, and a plateau appeared in the curve. At this stage, the measured displacement resulted primarily from the crack opening displacement. Note that the transverse displacement is not identical to the crack opening displacement until the stress reaches peak stress. For simplicity, however, the crack opening displacement in the present paper indicates the displacement between the two points at which a LVDT was mounted for all range of loading.

Once the measured displacement reached the predetermined cracked width, the specimen was unloaded. The slope of the curve during unloading was less steep than that during loading, which indicates the stiffness of the concrete was reduced due to the cracking. The degree of the stiffness reduction of concrete depended on the maximum crack opening displacement of the specimen (Figure 4). Here, stiffness of cracked concrete was defined as the slope of a line connecting two points with the stresses of 1 MPa and 3 MPa in the unloading curve. It was also noticed that after complete unloading, the crack opening displacement was reduced, i. e., the crack partially closed due to the material elasticity. The relationship between the crack recovery and the maximum crack opening displacement is shown in Figure 5. If a specimen was unloaded before reaching or even at the peak load, about 80% of the displacement could be recovered, and the remaining crack opening displacement would be very small. As a result, the crack may show little effect on concrete permeability, as measured on unloaded specimens.

Figure 4 Stiffness Reduction in Concrete due to Crack Openings

Figure 5 Recovery of Crack Opening Displacement (COD) after Unloading

Crack Patterns

To investigate the crack characteristics, some specimens were examined under an optical microscope with a magnification of 100x. The sequential crack patterns in the specimens with different crack widths were shown in Figure 6. It was noticed that the crack initiated in the center of a specimen where the uniform tensile stress was developed under the splitting load. The crack

grew toward the edge of the specimen as the measured crack opening displacement increased. Then, two main branch cracks were observed, and wedges formed due to the confinement of the concrete by the wood-bearing strips at the loading points. With further loading, additional fine cracks appeared and the main cracks jointed together. Although the specimen having a measured crack opening displacement of 900 microns did not break apart during the splitting test, it was too fragile to be handled for a permeability test.

Figure 6 Crack Patterns

The observed sequential crack patterns and measured crack openings provide us with important information on the crack characteristics in the concrete specimens. However, cracks may initiate from the surface of the specimens, and further study is needed to know if or when the cracks go completely through the thickness of a specimen.

Water Permeability Tests

A typical permeation curve obtained from water permeability tests is shown in Figure 7. The slope of a tangent line at a given point of the curve is directly proportional to the permeability coefficient of the concrete specimen at a given time of testing. It was observed that at the beginning of the test, the cumulative water flow increased non-linearly with time. After 20 days, water flow became steady and slower. The nonlinearity was likely due to the incomplete saturation of the specimen and unavoidable existence of air bubbles in the specimen, even though special care had been taken. The decreasing flow rate might also be due to the leaching of calcium from concrete and its precipitation with time. The leaching of calcium was observed during the curing of the concrete specimens under water.

Figure 7 A Typical Permeation Curve

Figure 8 Permeation Curves of Concrete Specimens with Different Crack Widths

Figure 8 shows the permeation curve of the concrete specimens with different cracks openings (prior to unloading). It was observed that for the concrete specimen having a crack opening displacement equal or smaller than 50 microns, the flow rates were very low. Therefore, the readings were taken once a day for the first week of testing, then reduced to once every two days or seven days so as to minimize the reading error in calculation of permeability coefficient. For the specimen with a cracking opening displacement of 180 microns, water flow rate was quite high. The reading had to be taken twice a day for the first few days of the test so as to prevent water from dropping below the readable marker on the pipette. The permeability coefficient, k, of a specimen with COD values less than 180 microns was calculated from the slope of the linear regression of the last part of its permeation curve. For specimens with cracking opening displacements of 350 and 550 microns, it took less than 2 minutes for water to drop from the top

to bottom of the pipette. The time of the water drop was recorded by a stopwatch, and the data provided for permeability coefficient calculation were based on the average of five flow rate measurements, which were very all close.

Figure 9 presents the relationship between water permeability and crack openings. It was observed that when specimens are loaded to crack opening displacements less than 50 microns, crack openings had little effect on concrete water permeability. When the crack opening displacement increased from 50 microns to about 200 microns, water permeability increased rapidly. With crack opening displacements larger than 200 microns, the rate of increase of water permeability becomes steady.

In addition to crack width, crack length and the number of cracks also influence concrete permeability. Figure 6 shows that the crack length and the number of cracks vary with predetermined crack opening displacements in the splitting tests. Appropriate methods are needed to gain accurate measurements of crack length, including microcracks, and the number of cracks in the whole area of the specimens.

Figure 9 Relationship Between Water Permeability and Crack Widths

Considering concrete deterioration due to the cracking, ACI Building Code (ACI 318-89 Commentary, Section 10.6) limits crack widths by limiting the distribution of flexural reinforcement in reinforced concrete design (7). The Code limitations are based on crack widths of 0.016 in. (400 μm) for interior exposure and 0.013 in. (330 μm) for exterior exposure, which are arbitrary numerical values from concrete practices. According to the present study, the permeability coefficient of concrete is about 10^{-3}~10^{-2} cm/sec when crack opening is about 300~400 μm, compared with 10^{-10}~10^{-9} cm/sec of uncracked concrete. With such high permeability, considerable leaking and corrosion of reinforcement may occur in the concrete structure during a limited service period. However, the cracks generated by the splitting tests may be the identical in widths on the inside as on the surface of the specimens, while the crack widths

adopted by the Code are surface crack widths and actual shear deformation of the concrete cover and curvature of flexural members will result in narrower crack widths at the level of the steel than at the surface, (i.e. V-shaped cracks). Further research is needed to study the effect of crack shape, specimen thickness, and tortuosity on permeability. The present study provides engineers with insight in developing design criteria for a durable concrete and in predicting service life of a concrete structure.

Summary and Conclusions

- The present research introduces feedback controlled splitting tests to generate width-controlled cracks in concrete specimens. This testing method has several advantages: 1) cracks are produced by tensile stresses, 2) crack opening displacement is recorded during loading and after unloading, and 3) the cylindrical specimens used in the loading tests are preferable for conventional concrete permeability tests.
- In this study, feedback controlled splitting tests were performed to obtain a series of concrete specimens with different crack widths. The results indicate that the crack opening displacement at the peak stress is less than 20 microns. At this loading level, about 80% of the displacement is recovered after unloading, and the remaining crack opening is very small, which may show little effect of cracking on concrete permeability.
- Water permeability of concrete with different crack widths was evaluated. The results indicated that concrete permeability increased with crack width. The degree of the permeability increase depends on the value of the crack opening in the concrete. When a specimen was loaded to have a crack opening displacement smaller than 50 microns, the crack opening had little effect on concrete permeability. When the crack opening displacement increased from 50 to 200 microns, concrete permeability increases rapidly. Beyond a crack opening displacement of 200 microns, the rate of increase of water permeability became constant.

Acknowledgments

This research is supported by NSF grant DMS9313013 to the National Institute of Statistical Sciences. Support from the NSF Center for Science and Technology of Advanced Cement Based Materials (ACBM) is also appreciated.

References

(1) P.K. Metha, Concrete Technology, Past, Present, and Future, Proc. of V. Mohan Malhotra Symposium, ed. by P.K. Mehta, ACI SP-144, p. 1-30, (1994)
(2) M. Saito, Cem. and Concr. Res. 25(4) 803 (1995)
(3) D. Ludirdja, R. L. Berger, and J. F. Young, ACI Mat. J. 86(5), 433 (1989)
(4) J. N. Cernica, Geotechnical Engineering: Soil Mechanics, John Wiley & Sons, p. 125 (1995)
(5) M. Tsukamoto, Darmstadt Concrete, Annual J. on Concr. and Concr. Str. 7 215 (1992)
(6) R. Gettu, B. Mobasher, S. Carmona, and D. Jansen, Adv. Cem. Based Mat. 3(2) 54 (1996)
(7) ACI Committee 318, "Building Code Requirement for Reinforced Concrete (ACI 318-89)", Am. Concr. Inst., Detroit, p. 106-108 (1989)

List of Figures

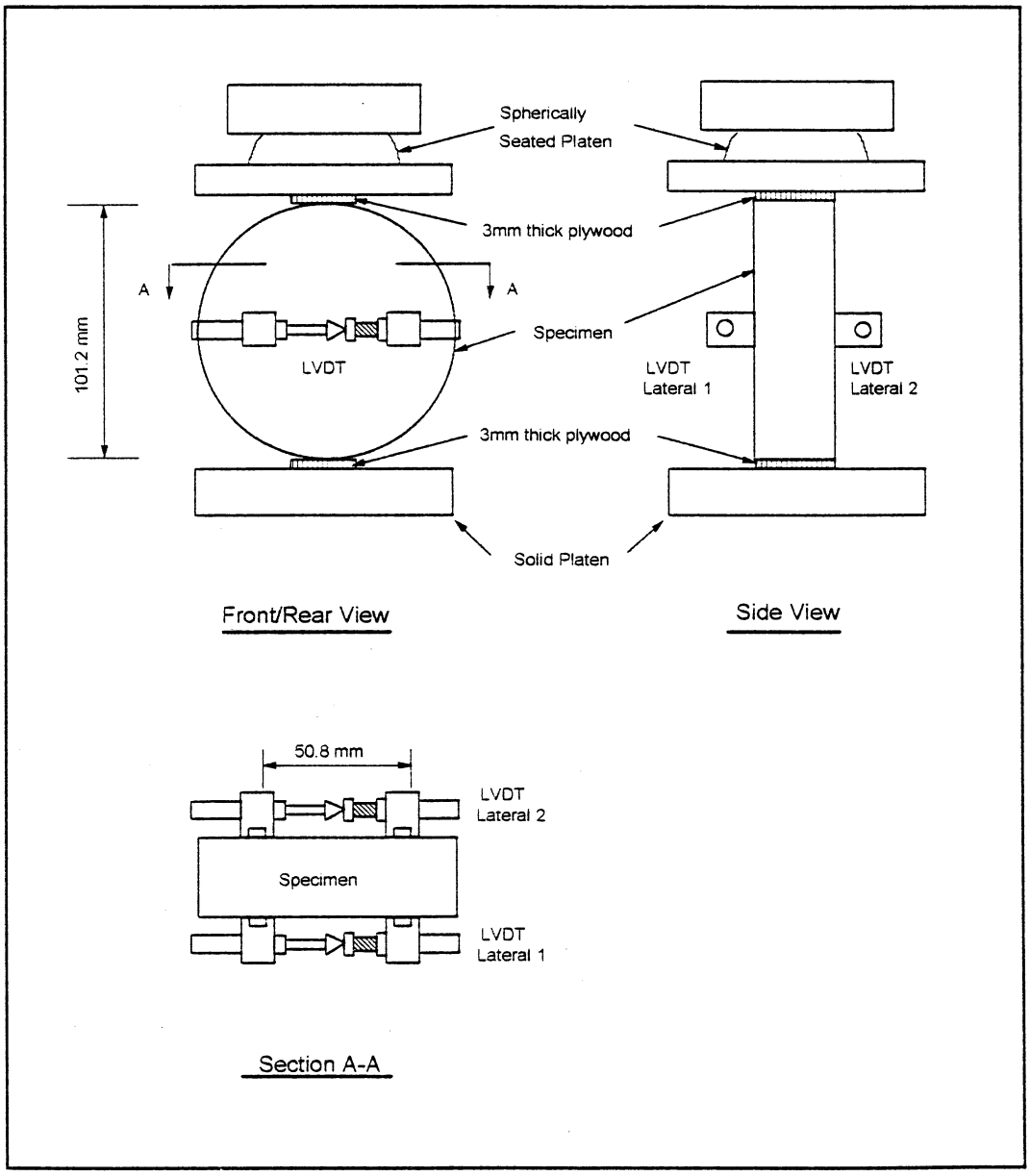

Figure 1 Feedback Controlled Splitting Test Setup

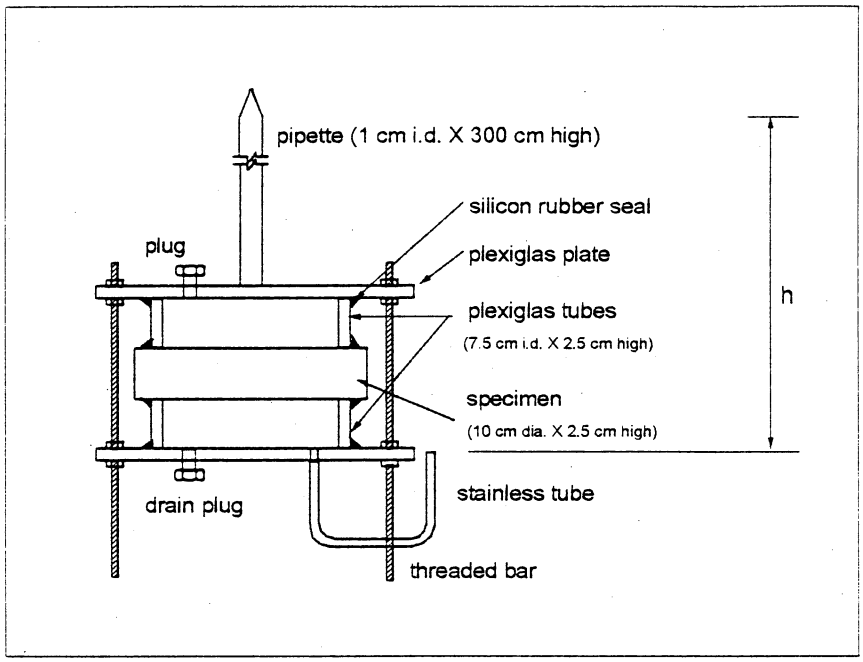

Figure 2 Schematic View of Water Permeability Apparatus

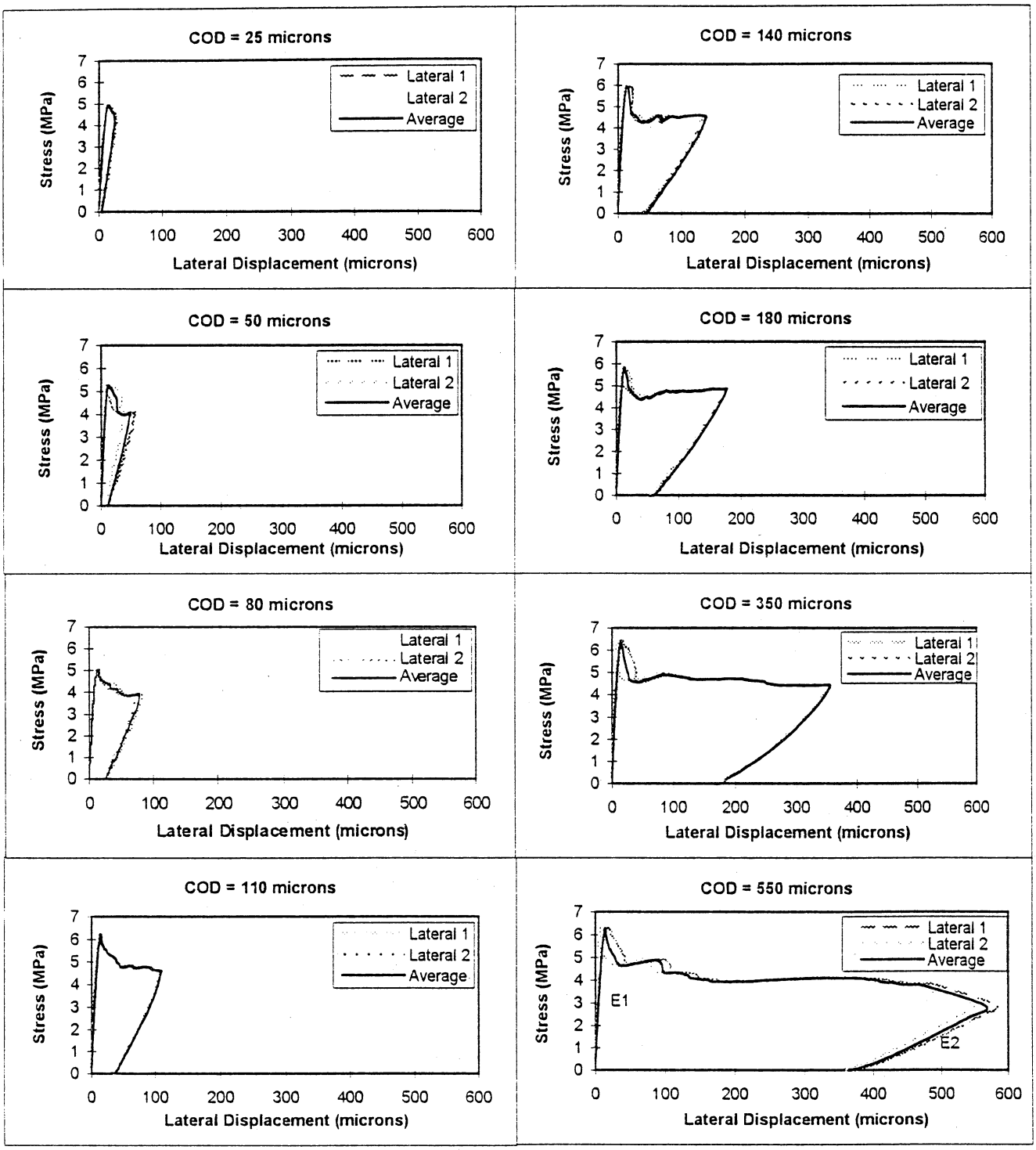

Figure 3 Results from Feedback Controlled Splitting Tests

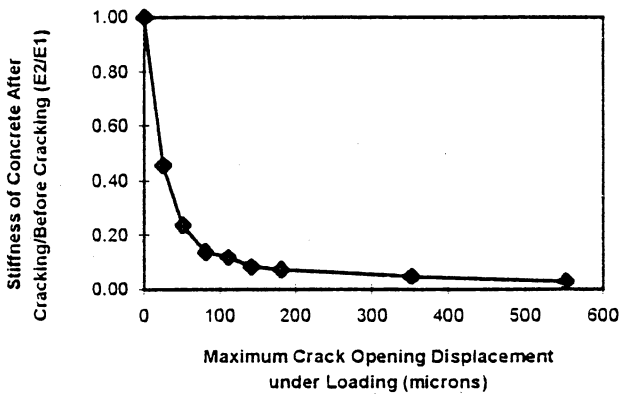

Figure 4 Stiffness Reduction in Concrete due to Crack Openings

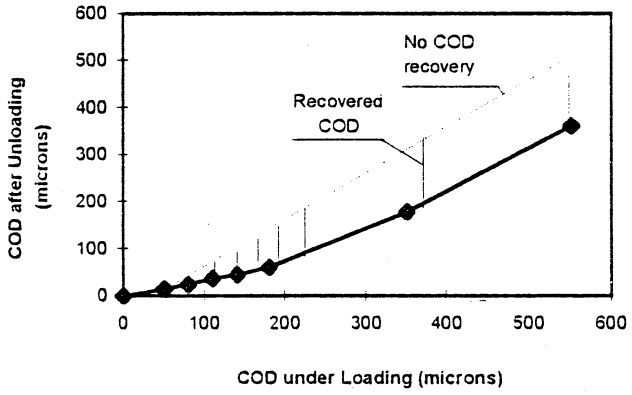

Figure 5 Recovery of Crack Opening Displacement (COD) after Unload

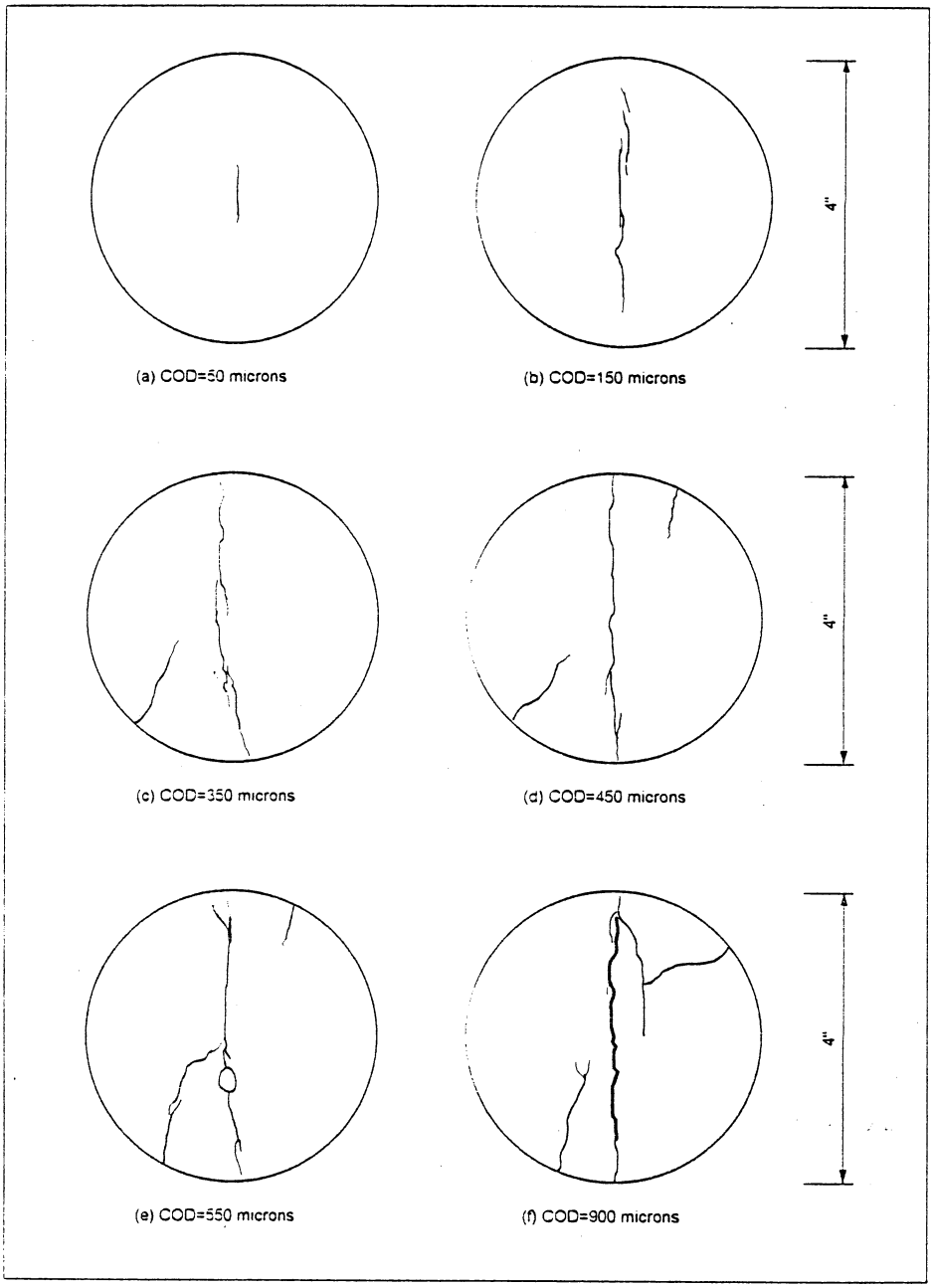

Figure 6 Crack Patterns

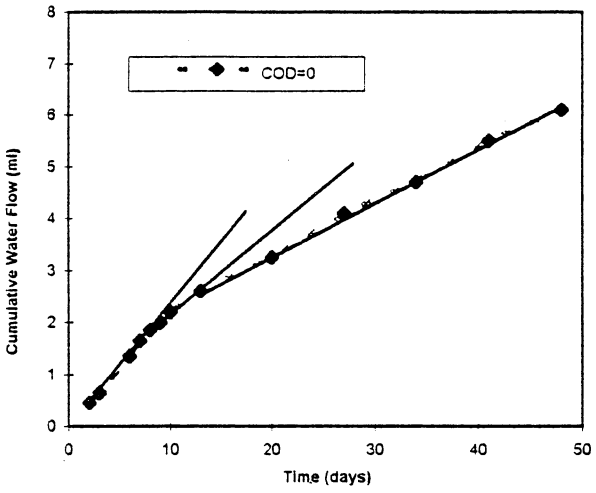

Figure 7 A Typical Permeation Curve

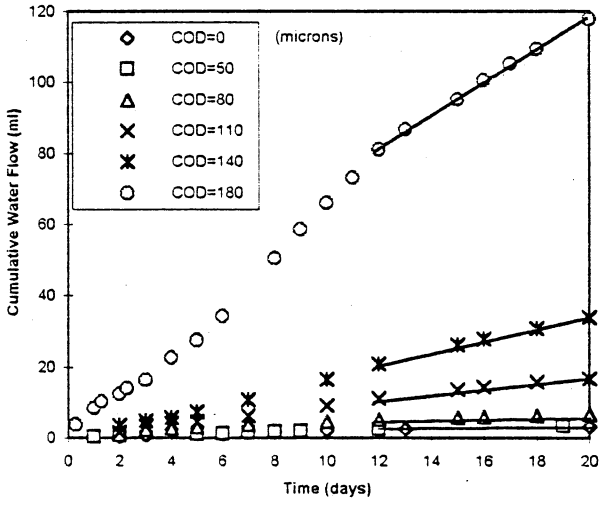

Figure 8 Permeation Curves of Concrete Specimens with Different Crack Widths

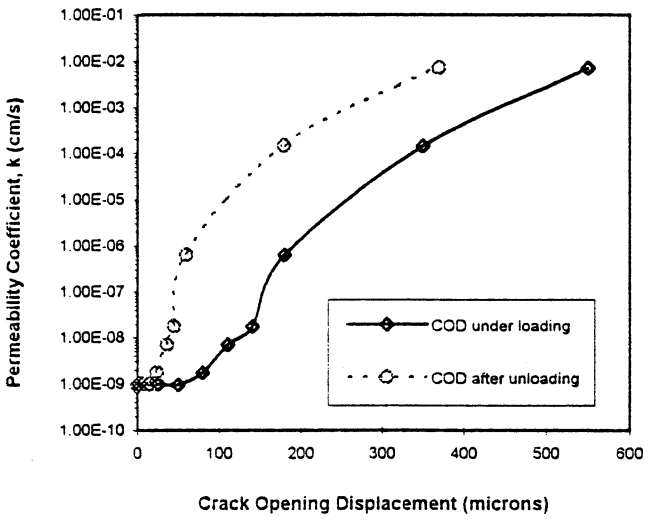

Figure 9 Relationship Between Water Permeability and Crack Widths